Divergent genetic mechanisms lead to spiny hair in mammals

Gislene L. Gonçalves[1,2*], Renan Maestri[1,3], Gilson R. P. Moreira[3], Marly A. M. Jacobi[4], Thales R. O. Freitas [1,2], and Hopi E. Hoekstra[5]

[1] Programa de Pós-Graduação em Genética e Biologia Molecular, Departamento de Genética, Instituto de Biociências, Universidade Federal do Rio Grande do Sul, Porto Alegre, RS, 91501-970, Brazil

[2] Departamento de Recursos Ambientales, Facultad de Ciencias Agronómicas, Universidad de Tarapacá, Arica, Chile

[3]Programa de Pós-Graduação em Biologia Animal, Departamento de Zoologia, Instituto de Biociências, Universidade Federal do Rio Grande do Sul, Porto Alegre, RS 91501-970, Brazil

[4] Departamento de Química. Universidade Federal do Rio Grande do Sul, Porto Alegre, RS 91501-970, Brazil

[5] Department of Organismic & Evolutionary Biology, Department of Molecular & Cellular Biology, Museum of Comparative Zoology, Howard Hughes Medical Institute, Harvard University, Cambridge, MA 02138, USA

Corresponding author:
Gislene L. Gonçalves
PPGBM, Departamento de Genética
Universidade Federal do Rio Grande do Sul
Porto Alegre, RS, 91501-970, Brazil
(+55 51) 3308-6726
lopes.goncalves@ufrgs.br

ABSTRACT

In humans, a single amino acid change (V370A) in the *Ecdysoplasin A receptor* (*Edar*) gene is associated with a unique hair phenotype in East Asian populations. Transgenic experiments in mouse show that this mutation enhances *Edar* signaling *in vitro,* which in turn alters multiple aspects of hair morphology. Here we tested whether this substitution contributes to the spiny hair observed in six families of rodents. We first measured hair traits, focusing on guard hairs and their physical properties, such as tension and deformation, and compared the morphology between spiny and non-spiny sister lineages. Two distinct hair morphologies were repeatedly observed in spiny rodent lineages: hairs with a grooved cross-section and a second near cylindrical form, which differ in their cross-section shape as well as their tensiometric properties. Next, we sequenced a portion of the *Edar* locus in these same species. Most species surveyed have the common amino acid valine at position 370, but the kangaroo rat and spiny pocket mouse have an isoleucine. We also found one additional amino acid variant: tree rats have a Leu^{422}Val polymorphism. However, none of these variants are associated with changes in hair morphology. Together these data suggest that the specific *Edar* mutation associated with variation in human hair morphology does not play a role in modifying hairs in wild rodents, highlighting that different evolutionary pathways can produce similar spiny hair morphology.

Key words: morphological evolution, EDAR, Rodentia, phylomorphospace

Running head: Evolution of spiny hair in mammals

Introduction

Hair is a defining trait of mammals yet can be highly differentiated among species, primarily with respect to density and morphology. For example, sea otters (*Enhydra lutris*) have the densest fur of any mammal, with up to 140,000 hairs/cm^2, more than on an entire typical human head[1]. A second extreme example is the modification of guard hairs into spines, which have evolved multiple times in mammals, including echidnas (Tachiglossidae), tenrecs (Tenrecidae), hedgehogs (Erinaceidae) and rodents (Hystricidae and Erethizontidae)[2]. In addition, a second type of spine, defined as aristiform hair[3], has evolved independently at least five times within Rodentia[2, 4, 5]. Yet, despite the many comparative descriptions of the structural features of hairs/spines, primarily for taxonomic studies in rodents[2, 4, 6-12], the evolutionary patterns and processes of morphological variation in these guard hairs is poorly understood. Similarly, identification of the genes and mutations underlying variation in hair structure is still nascent.

The role of the *Ectodysplasin A receptor* (*Edar*) gene, homolog to *Downless* in mouse [13], has been implicated in the morphological differentiation of hair and other ectodermic appendages in humans[14-17]. This gene encodes a novel member of the tumor necrosis factor (TNF) receptor family that include an extracellular cysteine rich fold, a single transmembrane region, and a death homology domain close to the C terminus[15, 18]. This transmembrane protein is a receptor for the soluble ligand *ectodysplasin A* (*Eda*) and can activate the nuclear factor-kappa B, JNK, and caspase-independent cell death pathways[19]. Mutations that inhibit this metabolic pathway prevent the formation of hair follicles in mice and humans[20-22], indicating the

involvement of this gene in development of hair, teeth, and other ectodermal derivatives[23].

In humans, a nonsynonymous SNP in the *Edar* gene, $T^{1540}C$ (rs3827760), causes a $Val^{370}Ala$ substitution and is associated with variation in hair structure in East Asian populations[24,25]. Transgenic experiments in mouse have shown that this specific mutation enhances *Edar* signaling *in vitro,* which in turn alters multiple aspects of its hair morphology including straighter hair fibers, increased diameter, and more cylindrical form compared to hair of either European or African origin[26]. Interestingly, this *Edar* mutant mouse has pelage that bears remarkable resemblance to that of wild mice with aristiform hairs, for example, the Southern African spiny mouse (*Acomys spinosissimus*). This gross-level phenotypic similarity led us to ask whether similar evolutionary pathways – at both the phenotypic and genetic levels – are responsible for the East Asian human hair phenotype and the spiny hairs observed in many rodent clades. Since *Edar* is a strong candidate for explaining variation in hair morphology, we have focused on this gene, and the $Val^{370}Ala$ mutation specifically.

In this study we investigate the hair phenotype in all six families of rodents that have spiny hairs (Table 1). First, we characterize their specific hair phenotype by comparing guard hairs ("spiny" and "control") between closely related species, focusing on variation in both morphology and physical properties such as size and shape as well as degree of tension and deformation. Second, we test for an association between genotype at the homologous amino acid position 370 in *Edar* and hair morphology. Together, these data allow us determine if spiny hairs have evolved through similar or different evolutionary pathways in humans and rodents.

Results

Variation in hair morphology

We uncovered substantial qualitative and quantitative variation in hair morphology among rodent species. While we found a gradient of shape in the cross sections of hairs, we could group the morphologies into three major forms: elliptical, grooved, and circular (Fig. 1), the latter two of which we considered "spiny" phenotypes. The non-spiny guard hairs of the three control species (i.e., kangaroo rat, gray brush-furred rat and deer mouse) were all elliptical and did not have a differentiated lateral groove or ridges (Fig. 1A-C). The grooved form varied dramatically, including spines with different degree of hardness. The spiny hairs present in the bristly mouse, spiny pocket mouse and Southern African spiny mouse are characterized by a pattern of crests on the dorsal surface and a decrease in the ventral curvature (Fig. 1D-I). Unlike the grooved hairs, medulla of the circular form in new world porcupines (Erethizontidae) have several uniform alveolar cells of small size and that fill the entire lumen, without septa and associated with an interleaved cortex of reduced thickness (Fig. 1J, K). Thus, spiny hairs, compared to control hairs, all share a dorsal groove associated with longitudinal side ridges, with the one exception of the New World porcupines (Erethizontidae) (Fig. 1D-I).

The grooved hair type was particularly abundant in our data set (6 of 11 taxa) and showed markedly differences among lineages. These hairs differed in length, width and thickness (Fig. 2). First, the Asiatic brush-tailed porcupine is the most distinct, having the widest hairs with a large area.

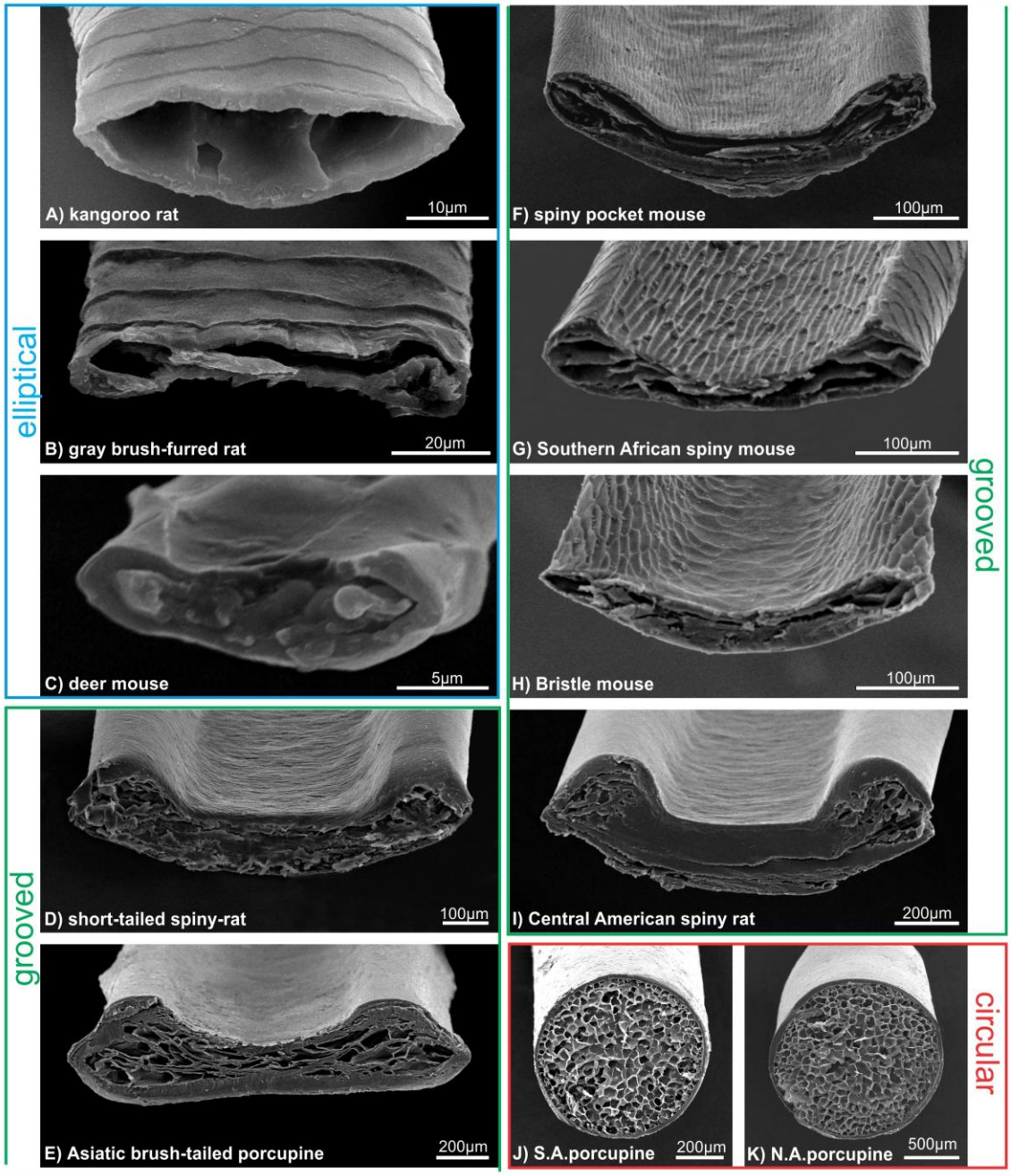

Figure 1. Scanning electron micrographs of cross sections of guard hairs, indicating the three major morphologies observed: elliptical (A-C), grooved (D-H) and circular (D-K).

Second, the short-tailed and Central American spiny rats had similar hair phenotype to each other with intermediate values – between the brush tailed porcupine and all other species – of length, width, thickness and area. Third, the spiny pocket mouse, Southern African spiny mouse and bristle mouse showed low values in length, width and thickness increase pattern. Therefore, a gradient from harder (Asiatic brush-tailed porcupine) to softer (the spiny pocket mouse, Southern African spiny mouse and bristle mouse) was evident within grooved hair type. We found an increase in the perimeter and cross-sectional area of softer spines compared to harder spines. We did not, however, find evidence of a homogeneous pattern in the degree of flatness across phenotypes (Fig. 2). The extent of concavity was similar between hairs with different degrees of hardness but significantly lower in the non-modified guard hairs of control species (deer mouse, gray brush-tailed rat and kangaroo rat).

The unique, hard spines observed in both species of New World porcupines (Erethizontidae) were both longer and thicker than any other taxa sampled (Fig. 2). The cylindrical shape of these spines (observed in cross section; Fig. 1J, K) resulted in a small perimeter/area ratio. Moreover, this cylindrical shape, and lack of groove and ridges, resulted in a flatness score near one and a concavity value of zero (Fig. 2).

To summarize the variation in hair morphology in a phylogenetic context, we plotted each species' mean hair shape in phylomorphospace. We found a remarkable degree of convergence in hair form among rodents with elliptical and grooved hair phenotypes (Fig. 3). Overall, PC1, which captures 72% of the variation, largely separates elliptical and circular hair shapes, and PC2 (22% of the variation) separates the grooved hairs.

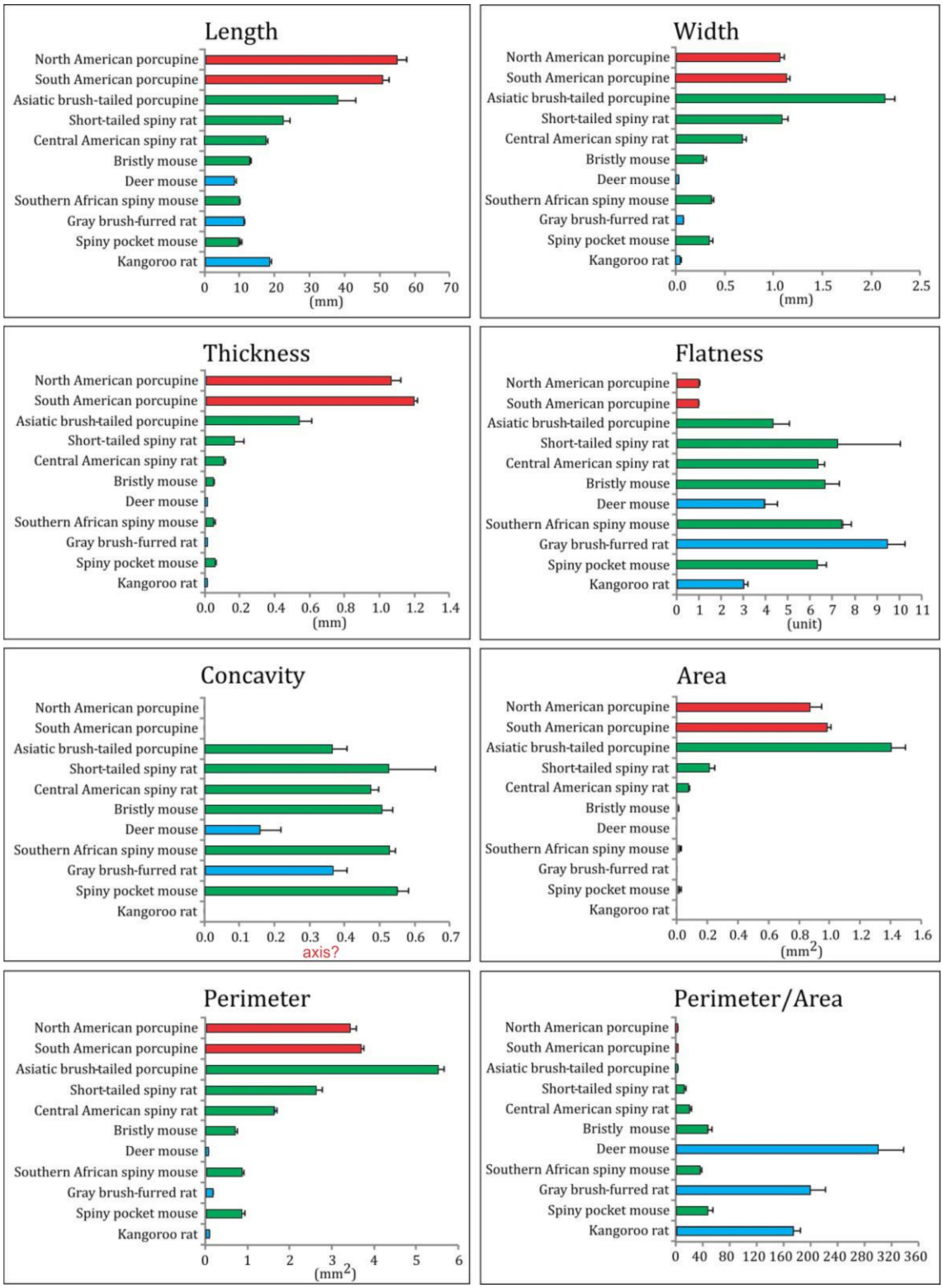

Figure 2. Variation in guard hairs among rodent species. Color indicates the cross-sectional morphology (as in Fig. 2). Sample size=10 specimens/species. Mean ± SE is provided.

Pairs of related species (within the families Heteromyidae, Cricetidae and Muridae) are separated in morphospace, reflecting their divergence in hair type despite their phylogenetic similarity. In other words, hair morphology does not closely reflect phylogenetic relationships, and other ecological factors, for example, are likely driving the observed morphological convergence.

Hair tension and deformation

To quantify how differences in hair morphology affect functional variation, we measured both hair tension and force as hairs were subjected to deformation. First, we found that the tension curves of non-spiny control species with elliptical hairs are distinct from the grooved and circular hairs (Fig. 4A). For elliptical hairs, tension can reach very high values (e.g. up to140 MPa) for the first 2-5% of deformation before the tension, σ, stabilized (around 20 MPa) and then, ultimately, the hair breaks. These elliptical hairs also show lower mechanical resistance (Fig. 4B). Grooved hair all had similar tensile curves, in which tension values increased in a roughly linear fashion for the first ~10% of hair deformation then slowly stabilized (Fig. 4A).

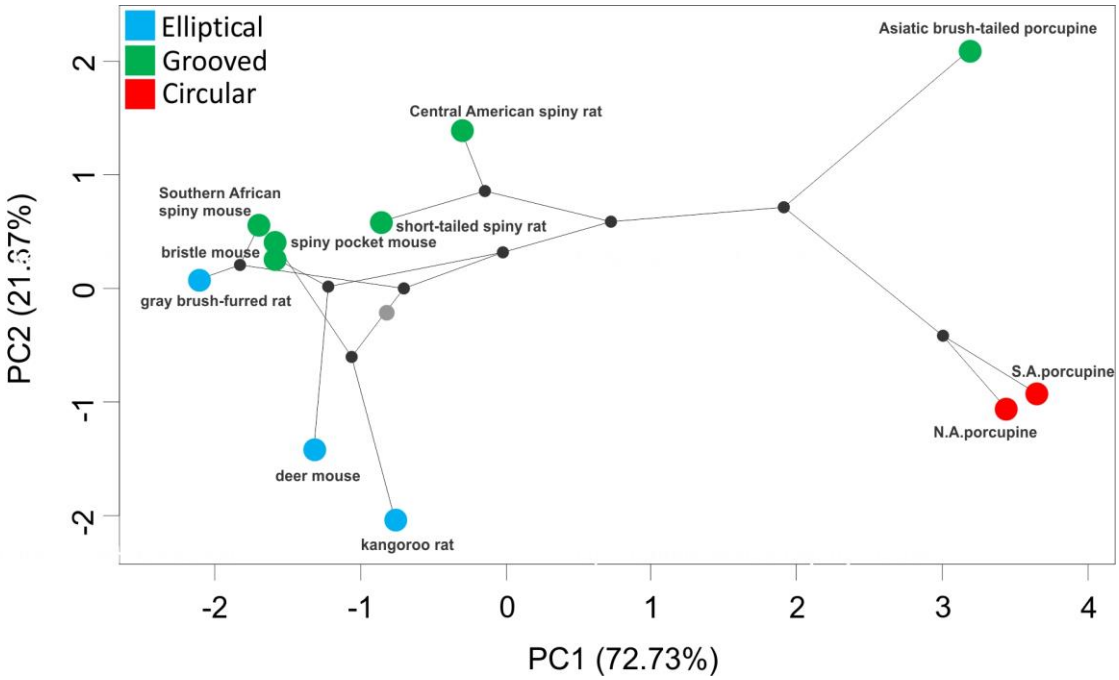

Figure 3. A phylomorphospace plot of hair morphology for 11 rodent species. Color indicates cross-sectional morphology: blue, elliptical; green, grooved; red, circular. A phylogeny based on cyt-*b* sequences is depicted on the morphological space. Nodes are represented by black dots, and the root by a gray dot.

Its maximum resistance—the peak in the curve after stabilization—was near the limit of deformation for most of these grooved species. Tension values were lower for the Asiatic porcupine and both the short-tailed and Central American spiny rats compared to the relative higher tension values of the grooved hair (Fig. 4A). The American porcupines (Erethizontidae) with circular hair shape have curves in which, after a shallow upward slope, tension remained constant over increasing deformation (Fig. 4A). Moreover, these spines also require the highest absolute force in our dataset needed to deform them (Fig. 4B). Thus, hair shape appears to affect both its tensile strength and the force required to deform the hair.

To measure the stiffness of hairs, we calculated the Young's elastic modulus, which describes tensile elasticity (or the tendency of an object to deform along an axis when opposing forces are applied along that axis). We found that elliptical hairs, of the non-spiny control species, had the highest values, indicating less stiff hairs, intermediate values for the grooved hairs, and the lowest values for the circular hairs of the porcupines (Fig. S1). One notable exception was the Asiatic porcupine, whose hairs had stiffness values similar to the New World porcupines, despite have grooved hair morphology. Thus, these data reinforce an overall pattern of convergence, in which similar hair morphologies have similar functional measurements.

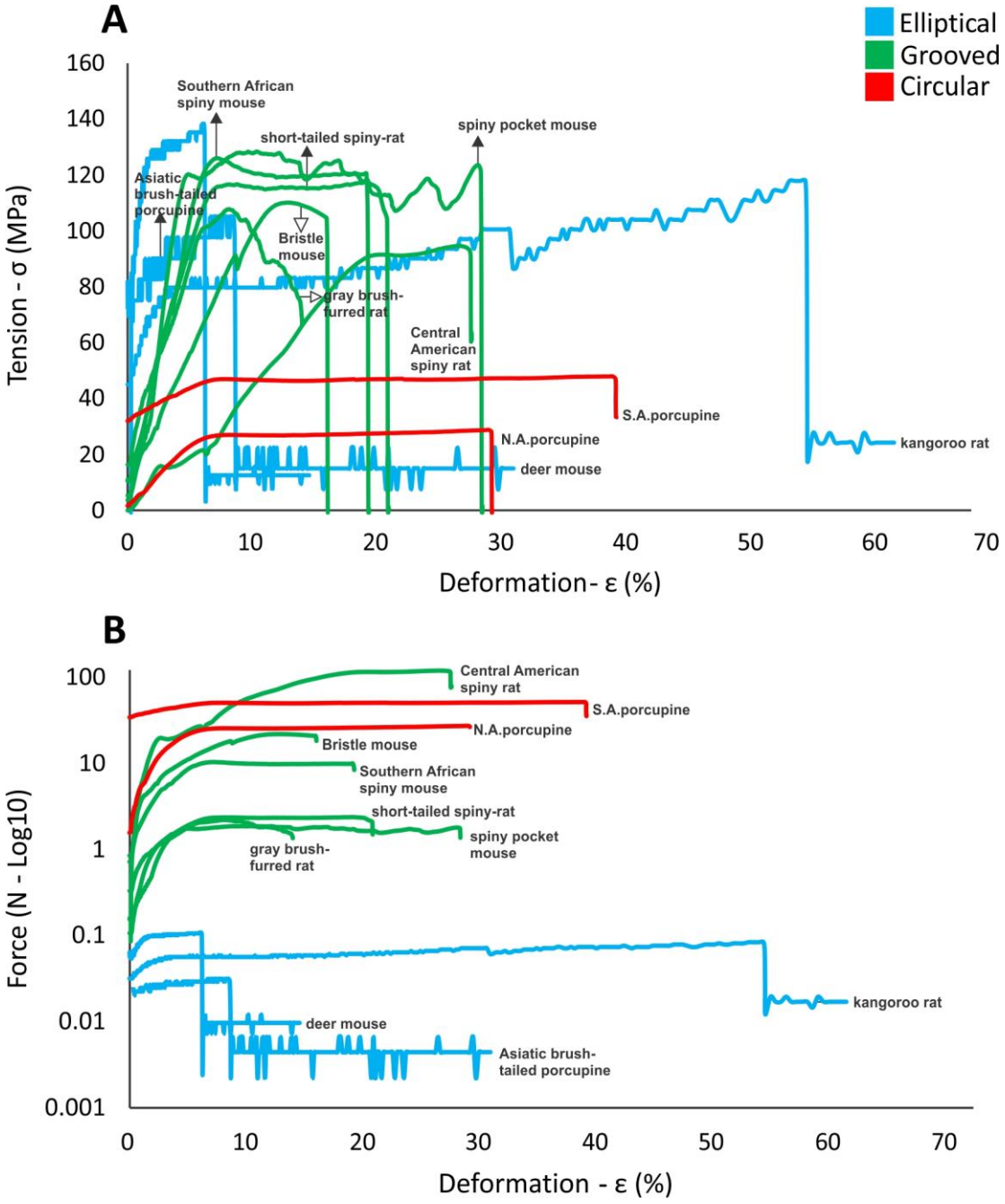

Figure 4. Deformation curves showing (**A**) tension and (**B**) force for hairs from 11 rodent species (labels correspond to species in Fig. 2).

Edar variants

To test for an association between hair phenotype and genotype, we sequenced 275 bp of the *Edar* gene in all 11 rodent species. Importantly, this segment spans exon 11 which contains the Val^{370}Ala mutation, previously implicated in hair differentiation in East Asian populations of humans. When comparing this region across these species, we observed a number of nucleotide substitutions (54 variable sites; Table S1), however most did not result in amino acid change. In fact, this region showed 98% amino acid conservation among these taxa (Fig. 5).

Most notably, the ^{370}Ala was not present in any rodent lineages, either spiny or non-spiny controls (Fig. 5). The first and third position of codon 370 did vary among species (whereas the second remained conserved), which resulted in one missense mutation (Val^{370}Iso), present in both the kangaroo rat (non-spiny phenotype) and the spiny pocket mouse (Fig. 5B). A second, conservative change at amino acid position 422 (Leu^{422}Val) was observed in only the tree rats, two closely related species. Thus, we found no obvious correlation between hair phenotype and the candidate amino acid change at position 370, and no new changes associated with hair morphology at other positions in the death domain of *Edar*.

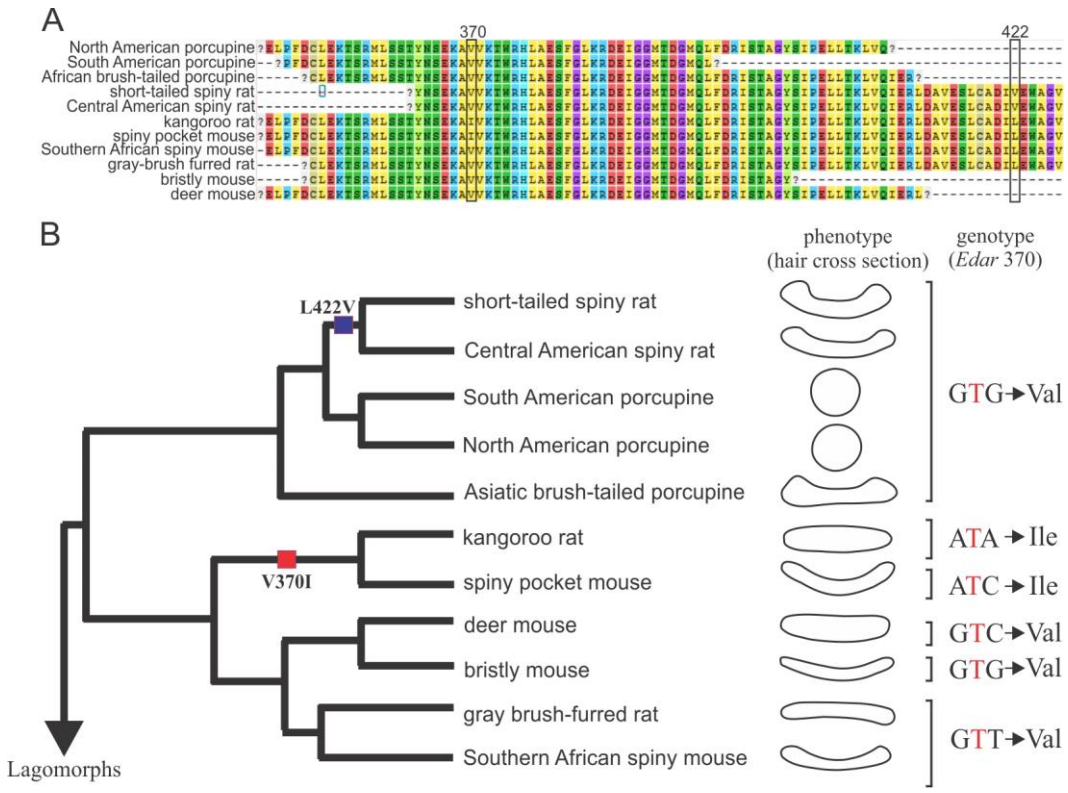

Figure 5. Amino acid sequence alignment of *Edar* gene, hair morphology and variability in 11 rodents. A) Variability along 275 bp of the last exon in *Edar* gene, indicating the two missense changes by squares. B) Bayesian phylogenetic tree reconstructed based on partial sequences of the cytochrome b gene. Two amino acid substitutions, $V^{370}I$ and $L^{422}V$, are mapped onto phylogeny. Hair morphology of each species is depicted by a cartoon of its cross section. Genotypes at the amino acid position 370 are indicated by the triplet of nucleotides.

Discussion

In this study, we clearly show that, at the level of morphology, two evolutionary pathways exist to make a hair spiny in wild rodents. Specifically, in the bristle mouse, spiny pocket mouse, Southern African spiny mouse, tree rats and Asiatic brush-tailed porcupine, a convergent pattern emerges: from a non-spiny ancestor hairs not only in increase in size (length, width and thickness) but also in the concave shape of cross-sectional area, mostly due to the presence of a dorsal groove. In addition, an increase in cortical medulla and the presence of transversal septa that acts as internal support was evident, as previously noted[2]. This earlier work suggested that the existence of a groove in these spiny hairs increased surface area, which, in addition to specific ultrastructural cuticle scales, in tropical and subtropical species likely played an important thermoregulatory (heat loss) and water condensation function. Moreover, the effect of increasing cross-sectional area and especially the cortical layer in reducing flexibility has been long recognized, at least for plant species[27]. Development of such grooves reduces torsion along the spine, an important characteristic associated with the effectiveness of spine penetration. These functions may explain the greater robustness and concavity as well as the relative increase in cortical area of spiny hairs compared to regular guard hair. Moreover, these traits are required for the function of this type of spine. In the Old World porcupine (*A. macrourus*), in which the spines have clear mechanical protective function[28], the tip is inserted in the body of predators during the defense according to the axial compression load. In this case, the entire retraction of the spine occurs. Alternatively, the tip, which is shorter and presents a

smaller cross-section (when compared to internal reinforcements) breaks and remain inside the body of predators[2].

A second evolutionary lineage corresponds to the circular section of spines present only in the New World porcupines (Erethizontidae). These circular and stiff spines have a morphology that maximizes the elastic buckling compared to the other five spiny rodent lineages studied. This biomechanical property is due to the small cross section relative to length, the lack of cortex, and the abundance of soft alveolar medulla that is continuous and without septa[29]. The penetration of this type of spine in the predator/opponent, which is deeper (compared to the previous case) is indeed initially associated with axial compression by buckling. Accordingly, the spine also breaks (but in a proximal region instead of the tip) and remains in the body[2]. The low-tension values indicated flexibility of this particular circular hair shape, in which stable and constant values of tension represent the greatest deformation without strain and breakage, making it ideal for predator defense – the spine is inserted with out it breaking. The Asiatic porcupine, and in a lesser degree the short-tailed and Central American spiny rats, have also strong hairs, and lower tension values compared to other spiny species (e.g., spiny pocket mouse, Southern African spiny rat, bristle mouse), which can also generate some flexibility, however significantly less than the American porcupines.

Thus, a spiny hair phenotype can be achieved in multiple ways. First, the concave hair of Asiatic porcupines likely represents a distinct evolutionary path from the American porcupines, even if facing similar ecological challenges. While American porcupines solves its predator challenge with greater flexibility (in which hair tension

values do not exceed 40 MPa until 30-40% of deformation), hair from the Old World porcupines have increased tension (around 100 MPa in the first 30% of deformation). Second, and contrary to our expectations, the two independent morphologies associated with spiny hairs of wild rodents are distinct from that of East Asian human populations[24, 25] and also the recently described *Edar* knock-out mouse model for the 370A allele[26]. In both Asians and Edar-/- mice, hairs showed an increase in thickness (=diameter), a straighter hair fiber and a circular cross-sectional profile compared to non-Asians or wild-type mice[16, 30].

As the detailed morphological shape and function of spiny hair observed in wild rodents were distinct from that of Asian humans, it was perhaps not surprising that the *Edar* 370A mutation was not present in any species surveyed, even in the New World porcupines that are morphologically most similar to Asian hair. We found several substitutions either in the first and third position of this 370 codon, regardless of the phenotypes, which resulted in one missense amino acid change ($Val^{370}Iso$). This mutation was present in both spiny and non-spiny phenotypes sister species (kangaroo rat and spiny pocket mouse), clearly consistent with a phylogenetic pattern rather than an association with spiny guard hairs. When we look across mammalian orders, we found that $Val^{370}Iso$ is also present in the lagomorph pika, the primate mouse lemur, and two lineages of marsupials, tasmanian devil and wallaby opossum, indicating that this codon was not conserved over evolutionary time. Another amino acid change ($L^{422}V$) was observed only in echimyid species. We were able to collect sequence data at this 422 site from only a few taxa (all non-spiny controls) because of its proximity to the end of the *Edar* death domain, which limits our ability to compare genotypes in other spiny rodents. However, when we again look across deeper divergence, we

found that guinea pig (a Hystricomorpha) also had the 422Val mutation. Moreover, we found this mutation in two other Hystricomorpha taxa (*Euryzygomatomys spinosus* and *Agouti paca*) (unpublished data). All these hystricomorph species show distinct degree of hardness of spiny hair. However, if this substitution is merely a neutral change in this lineage or involved in hair concavity, will require further comparative functional assays.

Despite the strong association between the *Edar* $V^{370}A$ variant and hair morphology in human populations with East Asian ancestry, some additional details should be considered. First, only one aspect of hair morphology, the ellipticity (ratio = thickness/diameter), was measured in humans. Other variables, such as cross-sectional size or shape, that can affect rigidity, for example, were not reported. Second, the specific mutation (1540C) identified in humans might not affect fitness, for example, differential survival, in other mammals. Although it is possible that an altered human hair phenotype was favored by natural or sexual selection, the selective pressure that acted on this SNP in East Asia populations is largely unknown[16, 24, 26]. Third, the cross-sectional shape observed by Mou et al. [26] in wild type mice differs from that observed for natural populations of *Mus musculus* (unpublished data). Thus, such association found in previous studies could be explained perhaps in part by the fact that different size and shape can be described for a given species, depending on the unit selected and the position of the cross sectional area[3]. These issues are important to consider when further probing the connection between *Edar* genotype and spiny-hair phenotype.

Although strongly associated with *Edar*, variation in hair thickness among human populations could not be explained exclusively by *Edar* 1540T/C (Fujimoto *et al*., 2008b), suggesting that other genetic variants associated with hair thickness. Genetic variants that affect the shape of hairs, in cross-sectional area or hair index, have yet to be identified. To identify other genes associated with hair morphology, Fujimoto et al.[31] examined an additional ten candidate genes: *Lef1, Msx2, Dll1, Egfr, Cutl1, Notch1, Fgfr2, Krt6irs, Gpc5, Akt1, Myo5a, Tgm3, Eda2R* and *Eda*. A significant association was observed in a G/T SNP (rs4752566) in the intron nine of the gene *Fgfr2*, which showed the strongest association with cross-sectional area and diameter size, even though in only one population investigated. These results suggest that other genes are likely involved in hair differentiation. Thus, either different mutations in the *Edar* gene or mutations in other genes likely contribute to the evolution of spiny-hair phenotypes in natural populations of mammals, including the rodents surveyed in this study.

In conclusion, our results show that, at a morphological level, there are at least two evolutionary paths that result in a spiny-hair phenotype in wild rodents. Compared to an elliptical shape of hairs in non-spiny rodents, we found hairs that were grooved in cross-section (in the bristle mouse, spiny pocket mouse, Southern African spiny mouse, tree rats and Asiatic brush-tailed porcupine) and an almost perfectly cylindrical form, present in the New World porcupines. These morphological types, in turn, lead to measurable differences in tensiometric properties, between each other and relative to non-spiny control mice as well as human hair. In addition, while a polymorphism in the *Edar* protein ($V^{370}A$) was associated with spiny hair morphology in human populations, all lineages of rodents included, independent of hair type, were fixed for Valine at position 370 of the *Edar* protein. Thus, the non-synonymous substitution in

the *Edar* gene previously associated with "spiny" hair morphology in humans does not play a role in modifying rodent hairs, suggesting different mutations in *Edar* and/or other genes are responsible for variation in the spiny hair phenotypes observed in wild rodent species.

Methods

We analyzed eight species that represent all six extant families of rodents that include at least one species with spiny hair: Spiny pocket mouse (*Heteromys desmarestianus*) [Heteromyidae], Southern African spiny mouse (*Acomys spinosissimus*) [Muridae], Bristly mouse (*Neacomys spinosus*) [Cricetidae], Short-tailed spiny rat (*Proechimys brevicauda*) and Central American spiny rat (*Proechimys semispinosus*) [Echimyidae], Asiatic brush-tailed porcupine (*Atherurus macrourus*) [Hystricidae], South American porcupine (*Sphiggurus villosus*) and North American porcupine (*Erethizon dorsatum*) [Erethizontidae] (Table 1). Within these six rodent families, we next identified closely related non-spiny taxa: Kangaroo rat (*Dipodomys panamintinus*) [Heteromyidae], Gray brush-furred mouse (*Lophuromys aquilus*) [Muridae] and Deer mouse (*Peromyscus maniculatus*) [Cricetidae], to control for the possible confounding effects of shared evolutionary history. Tissue samples from these 11 species were provided by the following museum collections: Museum of Comparative Zoology [MCZ], Harvard University; Museum of Vertebrate Zoology [MVZ], University of California, Berkeley; Field Museum of Natural History [FMNH]; National Museum of Natural History [NMNH], Smithsonian Institution; and Federal University of Rio Grande do Sul [UFRGS].

Table 1. Rodents specimens analyzed in this study.

Family	Species	Common name	Phenotype	Sample ID[a]
Heteromyidae	*Dipodomys panamintinus*	kangaroo rat	non-spiny (control)	BANGS 8426; MCZ 30157, 50896, MCZ 8427, 8469-8470, 10561-10563, 30155; MVZ-221901*
	Heteromys desmarestianus	spiny pocket mouse	spiny	BANGS 10714-10715; MCZ 10355, 10358, 28964 - 28966, 41298, 47300, 61799; MVZ-223183*
Muridae	*Lophuromys aquilus*	gray brush-furred mouse	non-spiny (control)	MCZ 43393-43402; FMNH-189129*
	Acomys spinosissimus	Southern African spiny mouse	spiny	NMNH 352823, 352828, 367023, 367158, 367080, 367092, 367124, 428798, 428825, 470462; FMNH-196233*
Cricetidae	*Peromyscus maniculatus*	deer mouse	non-spiny (control)	BANGS 1475-1479, 4803-4806, 7930; CRL8273*
	Neacomys spinosus	bristly mouse	spiny	MCZ 27061, 27357-27360, 27594, 38697-38700; MVZ-193762*
Echimyidae	*Proechimys brevicauda*	short-tailed spiny rat	spiny	MCZ 26936, 27368-27369; NMNH 259574, 559411-559412, 461334, 530937, 530939-530940; MVZ-190660*
	Proechimys semispinosus	Central American spiny rat	spiny	MCZ 10069-10073, 10075-10076, 10178-10179, 10185; MVZ-225062*
Hystricidae	*Atherurus macrourus*	Asiatic Brush-tailed porcupine	spiny	MVZ 14740, 18610, 23390, 24331, 32274, 32277-32281; MVZ-186559*
Erethizontidae	*Coendou spinosus*	South American porcupine	spiny	UFRGS- MRS15; MRS15*
	Erethizon dorsatum	North American porcupine	spiny	BANGS 1307, 1309, 2018, 2694, 5704, 6801; 6802, 7277; MCZ 655496-655497; JMC112*

[a]MCZ and BANGS: Museum of Comparative Zoology, Harvard University, USA; MVZ: Museum of Vertebrate Zoology, University of California, Berkeley, USA; FMNH: Field Museum of Natural History; NMNH: National Museum of Natural History, USA, Smithsonian Institution, USA; UFRGS: Universidade Federal do Rio Grande do Sul, Brazil.

*tissue sample

Morphometric analysis

For morphological analyses, we focused on guard hairs modified as spines and aristiforms hairs in the focal species and non-modified hairs in the phylogenetically-paired control species. Of the 11 taxa surveyed, we used a total of 10 specimens per species in the morphological and molecular analyses. All hairs were plucked from the lower left hip area to minimize differences due to pelage variation across the body. Hairs were gently removed with a pair of fine-tipped, self-closing forceps that caused no visible damage to the sample.

We first photographed each hair on a flat surface, and then cross-sectioned the hair with a scalpel and mounted the resultant sections on glass slides. We captured digital images, using a Sony Cyber-shot DSC-H10 digital camera attached to a stereomicroscope Leica M125 at the thickest point of each hair. We measured linear parameters, such as hair length, width, ellipticity and concavity (Fig. 6).

Cross-sectional ellipticity (*sensu* [26]) was calculated as a ratio of between width and thickness (= d/c), and concavity as the ratio between the depth of the dorsal groove (= zero, when absent) and cross section width (= b/d). We performed all hair measurements on digital images using AxioVision microscopy software (Zeiss).

To image the cross-sectional dimension of hairs using scanning electron microscopy, additional hairs were laid on a hard surface and cut transversally into 1-cm sections with a razor blade. Then, we mounted these sections with double-sided tape on metal stubs, coated with gold in a Bal-tec® SCD050 sputter coater to examine and photograph them using a JEOL® JSM6060 scanning electron microscope at the Centro de Microscopia Eletrônica (CME) of UFRGS.

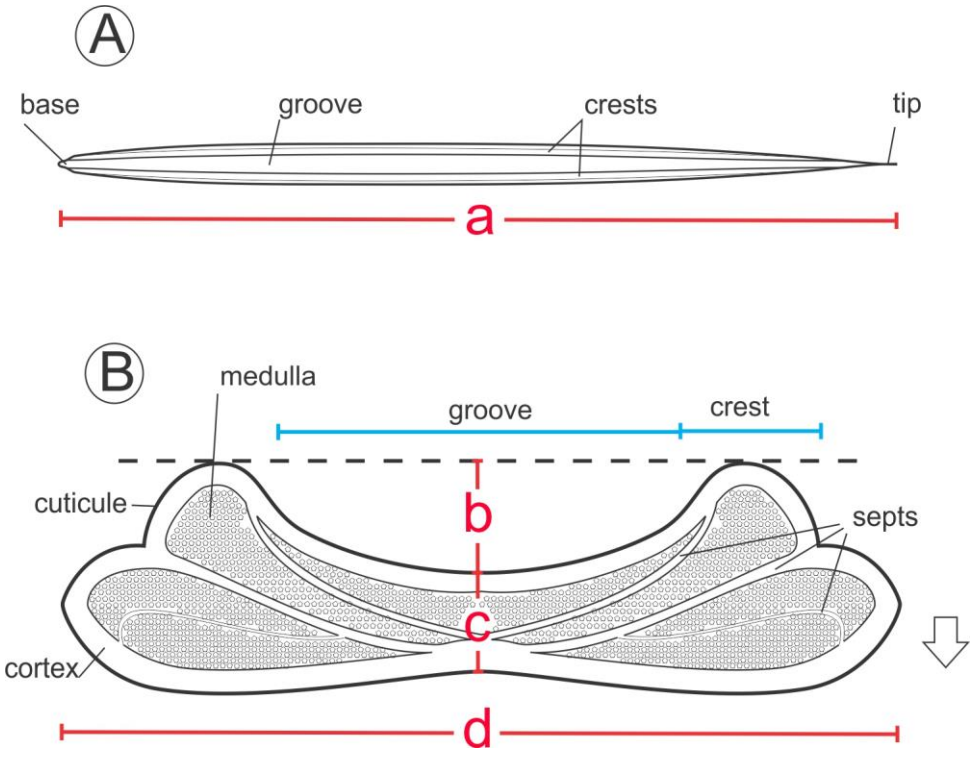

Figure 6. Schematic representation of a spiny hair showing (**A**) dorsal view and (**B**) cross section, with structural components. Measurements taken include: a = length, b = depth of groove, c = thickness, d = width. Arrow indicates the dorsal-ventral direction.

To describe the ultrastructure of hair surface, we employed nomenclature previously used[2], and for the shape of cross sections, we followed Teerink[3].

To detect evolutionary convergence and divergence, we visualized differences in hair shape among species using linear measurements to conduct a principal component analysis (PCA). A phylogenetic tree (see below) was projected onto the form space of the two first principal components, creating a phylomorphospace[32, 33]. Internal forms at nodes were reconstructed by squared-change parsimony. The phylomorphospace was created using phytools[34] in R[35].

Hair tension analysis

To generate hair tension values (σ) as function of the relative deformation (ε), we used a strain rate of 1mm/min on a universal testing machine EMIC DL 5000/10000. Next, to calculate the initial transversal area, the depth, and thickness of the flat samples and the radius for the cylindrical samples, we used a manual digital pachymeter with a precision of 0.01 mm. Specifically, we used a sample initial length (L_0) and load cell of 10mm and 500N, respectively, for the thicker hairs (porcupines), and 5 mm and 50N for the finer hairs. Samples were taken by using a razor blade, from the intermediate portion each individual hair, and had previously their distal portion glued with water putty (Durepox) to a small pieces of sand-paper (20 x 20 mm). This process increased friction, thus allowing stable anchoring of samples to the tension grips of the machine. From the force necessary to deform the sample, at a given time, until the rupture of the sample, expressed in Newtons (N) divided by the transversal initial area of the sample, A_o (A_0 = depth x thickness for the concave hair and $A_0 = \pi.r^2$

for the cylindrical samples, e.g., the New World porcupines), the tension, σ=N/Ao, was calculated and expressed by MPa (N/mm^2). The absolute relative deformation,ε is equal to $(L-L_0)/L_0$, a dimensional parameters, or expressed as a percentage (ε x100), L = the length of the sample at a given time, and L_0 = the initial length of the sample. The tensile strength as well the deformation are sensitive to macroscopic defects at the surface of the sample. For example, a catastrophic failure and a rapid propagation of the failure, normally, take place at a superficial defect of the sample. Consequently, from the initial ten samples measured for each species, we selected the best specimen to use in cross-species comparison. Within species variation was small, and thus using the best specimen helps to control for bias due to damaged or worn hair, as hairs form museum specimens were preserved in different conditions. Finally, by plotting tension as function of deformation, we generated the corresponding curves for each species.

In addition, to measuring hair stiffness, we calculated the Young's modulus, E = σ/ε in the linear deformation region, also designated as the elastic deformation region of a solid. It is a measure of the stiffness of the material and can be employed to compare the mechanical resistance of solid materials. In this study, the Young's modulus was calculated as slope of the curve, in the initial linear region of the curves (until 3% of deformation for all species). A bar plot comparing values of Young's modulus in a phylogenetic context was created using the phytools package in R.

Edar V370A polymorphism

For genetic analyses, we extracted total genomic DNA from tissue samples (muscle) preserved in DMSO using Blood and Tissue Kit (Qiagen) following manufacturer instructions. DNA was then stored at -20^{o}C. Degenerate primers were designed to amplify the final exon of *Edar* (Table 2), which encompass the variant V370A in humans. Importantly, this domain also plays a critical role in the recognition of the ligand *Edar* death domain. Because this is a highly conserved region[13], and several mutations were previously demonstrated to be involved in human clinical pathologies[36,37], substitutions in this region may be functionally relevant.

For the amplification reaction, we performed a touchdown PCR (i.e., decreasing annealing temperatures from 60 °C to 50 °C) with AmpliTaq Gold (Perkin Elmer) and 1.8 mM $MgCl_2$. We used primer pair F1+ R2 to amplify species in the Cricetidae, Heteromyidae and Muridae lineages and F2+R1 for Echimyidae, Erethizontidae and Hystricidae. We next verified the resultant PCR products in agarose gel stained with SybrSafe (Invitrogen), extracted the bands, and purified them using QIAquick Gel Extraction kit (Invitrogen). Using the same primer pairs, we next sequenced the fragments in both directions using BigDye chemistry in the automated sequencer ABI3730XL (Applied Biosystems).We next aligned all the sequence data using Codon Code Aligner (CodonCode Corp.).

To infer phylogenetic relationships among the rodents surveyed, we used a neutral mitochondrial DNA marker (cytochrome b [cytb]). For seven species, *cyt b* sequences were already available in GenBank (Supplementary Material); for three others, we sequenced a fragment of the gene (ca. 800 bp) using primers MVZ05 and MVZ16 with conditions described by Smith & Patton[37].

Table 2. Primers designed to amplify the 275-bp region of *Edar* gene associated with the death domain and encompassing the variant V370A.

ID	Sequence 5'→3'	Direction	Tm (°C)	GC content (%)
EDAR_F1	GTCTCAGCCCCACCGAGTTG	Forward	60.4	65.0
EDAR_F2	GYCTCAGCCCCACVGAGYTS	Forward	62.1	68.3
EDAR_R1	TCAGGACGCAGCTGGGGGTG	Reverse	64.7	70.0
EDAR_R2	TCAGGARGCAGCYGCCGVGG	Reverse	66.7	73.3

We constructed a phylogenetic tree using the maximum likelihood method with heuristic search option, tree bisection–reconnection, and an initial neighbor joining clustering. Branch support was estimated by 1000 bootstrap replications using a heuristic search of nearest-neighbor interchange.

Data Availability

The *Edar* sequence data generated and analyzed here are available from NCBI GenBank (MG780254-MG780264) and the corresponding author upon request**.**

References

[1] Kuhn, R. A., Ansorge, H., Godynicki, S. & Meyer, W. Hair density in the Eurasian otter *Lutra lutra* and the Sea otter *Enhydra lutris*. *Acta Theriologica* **55**, 211–222 (2010).

[2] Chernova, O. F. & Kuznetsov, G. V. Structural features of spines in some rodents (Rodentia: Myomorpha, Hystricomorpha). *Biology Bulletin* **28**, 371–382 (2001).

[3] Teerink, B. J. *Hair of West European Mammals: Atlas and Identification*. Cambridge: Cambridge University Press (1991).

[4] Hoey, K. A., Wise, R. R. & Adler, G. H. Ultrastructure of echimyid and murid rodent spines. *Journal of Zoology* **263**, 307–315 (2004).

[5] Wilson, D. E. & Reeder, D. M. *Mammal Species of the World: A Taxonomic and Geographic Reference*. Baltimore: Johns Hopkins University Press (2005).

[6] Schwarz, E. A new porcupine (*Thecurus*) from Borneo. *J. Mammalogy* **20**, 246–248 (1939).

[7] Po-Chedley, D. S. & Shadle, A. R. Pelage of the porcupine, *Erethizon dorsatum dorsatum*. *J. Mammalogy* **36**, 84–95 (1955).

[8] Findlay, G. H. Rhythmic pigmentation in porcupine quills. *Mammalian Biology* **42**, 231–239 (1977).

[9] Weer, D. J. Specific distinction in Old World porcupines. *Zoologische Garten* **53**, 226–232 (1983).

[10] Sokolov, V. E. & Chernova, O. F. New data on structure of quills in Hystricomorpha (Rodentia). *Rossijskaya Akademii Nauk* **363**, 429–432 (1998).

[11] Chernova, O. F. Evolutionary aspects of hair polymorphism. *Biology Bulletin* **33**, 43–52 (2006).

[12] Duarte, T. S. *Micromorfologia de pelos aristiformes de roedores das famílias Cricetidae e Echimyidae (Mammalia: Rodentia).* MSc Thesis. Universidade Federal de Viçosa, 52p, *in Portuguese* (2013).

[13] Pantalacci, S., Chaumot, A., Benoît, G., Sadier, A., Delsuc, F., Douzery, E. J. *et al.* Conserved features and evolutionary shifts of the EDA signaling pathway involved in vertebrate skin appendage development. *Mol Biol Evol* **25**, 912-928 (2008).

[14] Garcin, C. L., Huttner, K. M., Kirby, N., Schneider, P. & Hardman, M. J. Ectodysplasin A pathway contributes to human and murine skin repair. *J Invest Dermatol* **136**, 1022–1030 (2016).

[15] Mikkola, M. L. & Thesleff, I. Ectodysplasin signaling in development. *Cytokine Growth Factor Review* **14**, 211–224 (2003).

[16] Kamberov, Y.G., Wang, S., Tan, J., Gerbault, P., Wark, A., Tan, L. *et al.* Modeling recent human evolution in mice by expression of a selected *EDAR* variant. *Cell* **152**, 691–702 (2013).

[17] Kamberov, Y. G., Karlsson, E. K., Kamberova, G. L., Lieberman, D. E., Sabeti, P. C., Morgan B. A. *et al*. A genetic basis of variation in eccrine sweat gland and hair follicle density. *Proc Natl Acad Sci USA* **112**, 9932–9937 (2015).

[18] Headon, D. J., Overbeek, P. A. Involvement of a novel *Tnf* receptor homologue in hair follicle induction. *Nature Genetics* **22**, 370–374 (1999).

[19] Kumar, A., Sinha, S., Jasmin, A., Chaudhary, P. M. The ectodermal dysplasia receptor activates the nuclear factor-kappaB, JNK, and cell death pathways and binds to ectodysplasin A. *Journal of Biological Chemistry* **276,** 2668–2677 (2001).

[20] Thesleff, I., Mikkola, M. L. Death receptor signaling giving life to ectodermal organs. *Science STKE: Signal Transduction Knowledge Environment,* **131**, PE22 (2002).

[21] Botchkarev, V.A. & Fessing, M.Y. Edar signaling in the control of hair follicle development. *Journal of Investigative Dermatology Symposium Proceedings* 10:247–251 (2005).

[22] Courtois, G. & Smahi, A. NF-kappaB-related genetic diseases. *Cell Death and Differentiation* **13**, 843–851 (2006).

[23] Masui, Y., Farooq, M., Sato, N., Fujimoto, A., Fujikawa, H., Ito, M. *et al*. A missense mutation in the death domain of *EDAR* abolishes the interaction with EDARADD and underlies hypohidrotic ectodermal dysplasia. *Dermatology* **223**, 74-79 (2011).

[24] Fujimoto, A., Kimura, R., Ohashi, J., Omi, K., Yuliwulandari, R., Batubara, L., *et al*. A scan for genetic determinants of human hair morphology: EDAR is associated with Asian hair thickness. *Human Molecular Genetics* **17**, 835–843 (2008a).

[25] Fujimoto, A., Ohashi, J., Nishida, N., Miyagawa, T., Morishita, Y., Tsunoda, T. *et al*. A replication study confirmed the *EDAR* gene to be a major contributor to population differentiation regarding head hair thickness in Asia. *Human Genetics* **124**, 179–185. (2008b).

[26] Mou, C., Thomason, H. A., Willan, P. M., Clowes, C., Harris, W. E., Drew, C. F. *et al*. Enhanced ectodysplasin-A receptor (EDAR) signaling alters multiple fiber characteristics to produce the East Asian hair form. *Human Mutation* **29,** 1405-1411 (2008).

[27] Rusu, M., Mörseburg, K., Gregersen, O., Yamakawa, A. & Liukkonen, S. Relation between fibre flexibility and cross-sectional properties. *BioResources* **6**, 641-655 (2011).

[28] Hausman, L. A. Structural characteristics of the hair of mammals. *American Naturalist* **54**, 496–523 (1920).

[29] Karam, G. N. & Gibson, L. J. Elastic buckling of cylindrical shells with elastic cores. I–analysis. *International Journal of Solids Structures* **32**, 1259-1283 (1995).

[30] Bryk, J., Hardouin, E., Pugach, I., Hughes, D., Strotmann, R., Stoneking, M. *et al*. Positive selection in East Asians for an *EDAR* allele that enhances NF-kB activation. *PLoS One* 3, e2209 (2008).

[31] Fujimoto, A., Nishida, N., Kimura, R., Miyagawa, T., Yuliwulandari, R., Batubara, L. *et al. FGFR2* is associated with hair thickness in Asian populations. *Journal of Human Genetics* **54**, 461–465 (2009).

[32] Klingenberg, C. P & Ekau, W. A combined morphometric and phylogenetic analysis of an ecomorphological trend: pelagization in Antarctic fishes (Perciformes: Nototheniidae). *Biological Journal of the Linnean Society* **59**, 143–177 (1996).

[33] Sidlauskas, B. Continuous and arrested morphological diversification in sister clades of characiform fishes: a phylomorphospace approach. *Evolution* **62**, 3135–3156 (2008).

[34] Revell, L. J. phytools: An R package for phylogenetic comparative biology (and other things). *Methods in Ecology and Evolution* **3**, 217-223 (2012).

[35] R Core Team. R: A language and environment for statistical computing. R Foundation for Statistical Computing, Vienna, Austria. URL https://www.R-project.org/ (2017).

[36] Sabeti, P. C., Varilly, P., Fry, B., Lohmueller, J., Hostetter, E., Cotsapas, International HapMap Consortium *et al*. Genome-wide detection and characterization of positive selection in human populations. *Nature* **449**, 913–918 (2007).

[37] Smith, M. F. & Patton, J. L. Diversification of South American muroid rodents: evidence from mitochondrial DNA sequence data for the Akodontine tribe. *Biological Journal of the Linnean* Society **50**, 149-177 (1993).

Acknowledgements

We thank to Judith Chupasko (MCZ, Harvard University), Chris Conroy (MVZ, University of California, Berkeley), Ingrid Rochon (Smithsonian Institution, National Museum of Natural History) and Bruce Patterson (Field Museum of Natural History) for kindly providing DNA samples and loans of rodent hairs. We also thank the Electron Microscopy Center at UFRGS for use of the micrograph equipment. This work was supported by the American Society of Mammalogists (Grant-in-Aid), the Coordenadoria de Aperfeiçoamento de Pessoal de Nível Superior (CAPES), the Conselho Nacional de Desenvolvimento Científico e Tecnológico (CNPq), and the National Science Foundation (DEB-0919190). G.L.G. and R.M. received a postdoctoral fellowship from CNPq (processes 500745/2011-0 and 150391/2017-0, respectively). H.E.H. is an Investigator of the Howard Hughes Medical Institute.

Author information

Affiliations

Programa de Pós-Graduação em Genética e Biologia Molecular, Departamento de Genética, Universidade Federal do Rio Grande do Sul – Av. Bento Gonçalves, 9500, CEP 91501-970, Porto Alegre, RS, Brazil

Gislene L. Gonçalves & Thales R. O. Freitas

Departamento de Recursos Ambientales, Facultad de Ciencias Agronómicas, Universidad de Tarapacá, Arica, Chile

Gislene L. Gonçalves

Programa de Pós-Graduação em Biologia Animal, Departamento de Zoologia Universidade Federal do Rio Grande do Sul, Av. Bento Gonçalves 9500, 91501-970, Porto Alegre, Brazil

Renan Maestri, Gilson R. P. Moreira & Thales R. O. de Freitas

Departamento de Química, Universidade Federal do Rio Grande do Sul, Av. Bento Gonçalves 9500, 91501-970, Porto Alegre, Brazil

Marly A. M. Jacobi

Department of Organismic & Evolutionary Biology, Department of Molecular & Cellular Biology, Museum of Comparative Zoology, Howard Hughes Medical Institute, Harvard University, Cambridge, MA 02138, USA

Hopi Hoekstra

Contributions

G.L.G. and H.E.H. conceived and designed the experiment. R.M., G.R.P.M. and T.R.O.F. performed the morphometric analyses. M.A.M.J. performed hair tension experiment

and together with R.M. and G.R.P.M. analyzed the data. G.L.G, R.M, and G.R.P.M wrote the manuscript, with input from all authors.

Competing Interests

The authors declare that they have no competing interests.

Electronic supplementary material

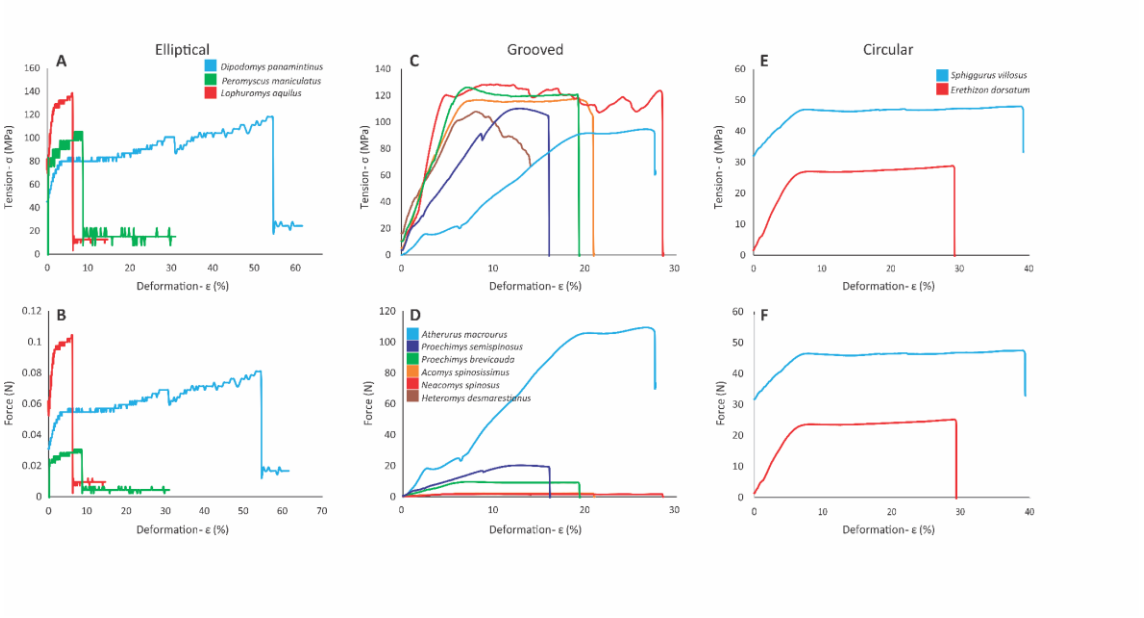

Figure S1 Deformation curves in relation to tension (A, C, E) and force (B, D, F) for hairs of eleven rodent species, split according to the cross-section shape of the hair.

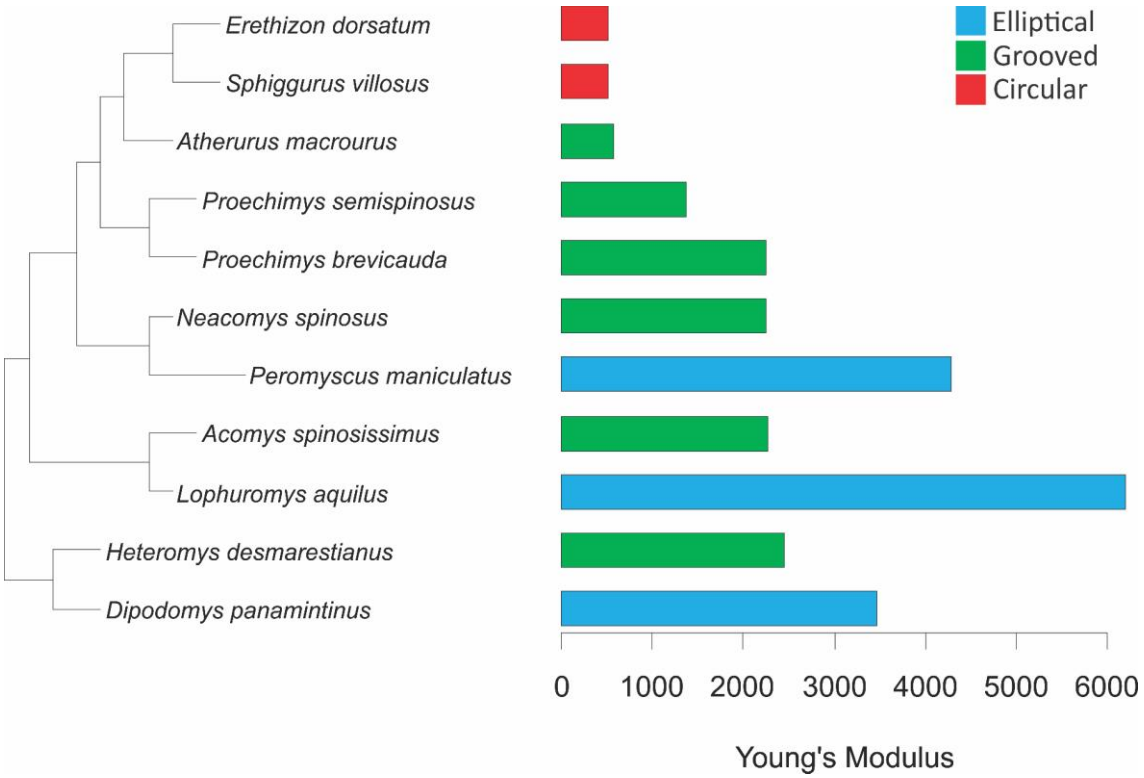

Figure S2. Young's modulus for the linear portion of hair deformation curves (Fig.5A) for eleven rodent species. The modulus was calculated as $E = \sigma/\varepsilon$ for the initial portion of each deformation curve (at 3% of deformation).